

Unsaturated flow processes are often both non-linear and discrete in nature such as the wetting front in Figure 1. Thus, local moisture measurements and accurately locating the wetting front become a key factor in analysis. Laboratory studies in unsaturated soil are often limited in the number of measurement points due to spatial or cost limitations. Complementary numerical studies provide insight to intermediate behavior, however, the non-linear inputs (storage function, unsaturated conductivity function) make a unique solution challenging to produce. Unsaturated transparent soil (Peters et al. 2011, Sills et al. 2017) allows for direct observation and measurement of the degree of saturation regime for continuous and discontinuous experiments at high spatial and temporal resolution. A digital image from an infiltration experiment is shown in Figure 1, which displays a descending wetting front migrating through initially dry soil. Above the wetting front the soil is dark, which is contrasted with the white appearance for dry soil. Unsaturated transparent soil experiments are performed in Perspex apparatuses allowing for digital images to be captured. In Figure 1, the wetting front is easily observable allowing for accurate measurement of its location. In addition to locating the wetting front, degree of saturation measurements between 0 and 100% are made through a digital image analysis scheme first reported by Peters et al. (2011). Later Siemens et al. (2013) and (2014) presented infiltration experiments and numerical simulations that examined the effect of air drainage on the mobility of the wetting front and the degree of saturation within the transmission zone of homogenous and layered profiles. Recently Sills et al. (2017) examined visualization theory, developed rigorous degree of saturation calibration methodology and a new calibration function, which has the advantage of being continuous.

Unsaturated flow studies are limited in the number of measurement points due to cost as well as spatial constraints. Unsaturated transparent soil has previously displayed the potential for providing continuous degree of saturation measurements across laboratory experiments. There are theoretical and practical limitations on the obtainable spatial resolution of saturation measurements, which are dependent on the soil properties, digital camera capabilities, and image processing expertise. In this paper, the image processing method for unsaturated transparent soil experiments is presented and guidance in selecting a spatial resolution is provided.

MATERIALS AND METHODS

Transparent soil is formed by matching the refractive indices of a soil and saturating fluid. Unsaturated transparent soil, for these studies, is formed by a fused quartz and mineral oil mixture with details found in Peters et al. (2011), Siemens et al. (2013, 2014) and Sills et al. (2017). At $S_r=100\%$, the soil is transparent and at $S_r=0\%$ the soil is white. Between these extremes, unsaturated transparent soil changes color as shown in Figure 1. The fused quartz used at Royal Military College of Canada is

found in two gradations, termed coarse and fine. Characteristic grain-sizes for transparent soil are d_{10} , d_{30} , and d_{60} of 0.75, 1.16, and 1.175 mm for the coarse gradation and 0.13, 0.27, and 0.45 mm for the fine gradation respectively. The fused quartz has a specific gravity of 2.3 and refractive index of 1.459. The wetting fluid is composed of a mineral oil mixture of Petro-Canada Krystol 40 and Life Brand baby oil, which is combined to give a refractive index of 1.459. The mineral oil mixture has a liquid density of 0.83 Mg/m^3 , surface tension of 0.023 N/m at 22°C and viscosity of 0.01 kg/(m s) at 25°C .

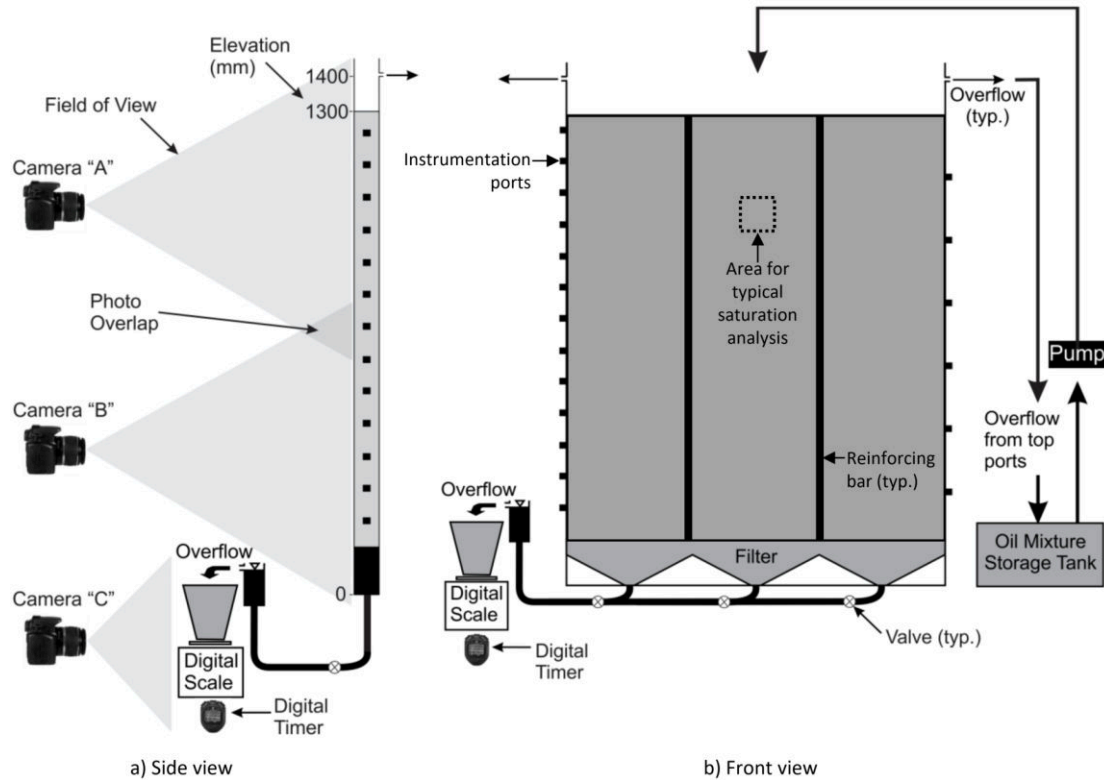


Figure 2. Schematic of transparent soil apparatus.

The flow apparatus used for two-dimensional applications is shown schematically in Figure 2 (Siemens and Oldroyd 2014). The flow apparatus is constructed of Perspex with internal dimensions $1.2 \text{ m} \times 1.4 \text{ m} \times 0.045 \text{ m}$ (width/height/thickness). The apparatus is placed in front of a black background so that the soil appears dark when saturated, which contrasts the light color at $S_r=0\%$. Hydraulic boundary conditions are controlled at the top, bottom, and sides allowing for infiltration and rainfall at the surface, open and closed air drainage along the sides and phreatic surface control at the base. Three digital SLR cameras are placed in front of the apparatus to simultaneously capture images of unsaturated transparent soil experiments such as the one highlighted in Figure 1. Digital images are captured at time intervals as low as 5s,

which allows for high temporal and spatical resolution of degree of saturation measurements.

DIGITAL IMAGE ANALYSIS

The process for converting digital images to degree of saturation measurements is summarized in Figure 3, which is using the area highlighted in Figure 1 as an example. Before an infiltration experiment is performed, the dry ($S_r=0\%$) and saturation ($S_r=100\%$) images are captured. The camera settings are selected such that the widest practical range of pixel intensities between the dry and saturation images (maximum 255) is captured. Ceiling lighting inherently causes changes in pixel intensity along the height of the apparatus so this effect is considered when selecting camera settings. In the bounding images shown in Figure 3, the average difference in pixel intensity between the saturation and dry images is 150-170, which is comparable to Peters et al. (2011). Once the dry and saturation images are captured, camera settings and locations are held constant for further experiments.

During unsaturated transparent soil experiments, numerous digital images are captured during test preparation, conduction, and de-construction. Following experiments, the images are scrutinized for temporal lighting variation, which would alter the saturation measurements. Image processing begins by performing geoPIV (White et al. 2003) on all images to correct for camera movement between the dry, saturation, and experimental images. Along with aligning images, the (x,z) coordinates of every pixel is determined. The analysis area highlighted in Figure 1 is shown in Figure 3 between the dry and saturation images to display the image processing technique. First, each experimental image is grey-scaled and then the normalized pixel intensity is calculated at the pixel resolution as:

$$I_N(x, z) = \frac{I_D(x,z) - I(x,z)}{I_D(x,z) - I_S(x,z)}$$

where I_N = normalized pixel intensity, I_D = pixel intensity of the dry image, I = pixel intensity of the current experimental image, I_S = pixel intensity of the saturation image, x,z = coordinate system. This produces a normalized pixel intensity image where $I_N=0$ corresponds to $S_r=0\%$ and $I_N=1$ corresponds to $S_r=100\%$. Finally, the normalized intensity images are converted to degree of saturation images using Sills et al. (2017) equation:

$$S_r(x, z) = \left\{ \frac{-0.95}{\ln(0.07)} \ln(I_N(x, z)) \right\} S_r(x, z) = \left\{ \frac{-0.95}{\ln(0.07)} \ln(I_N(x, z)) \right\} + 1$$

with the saturation image displayed at the bottom of Figure 3. This process is applied to every experimental image captured during an unsaturated flow experiment.

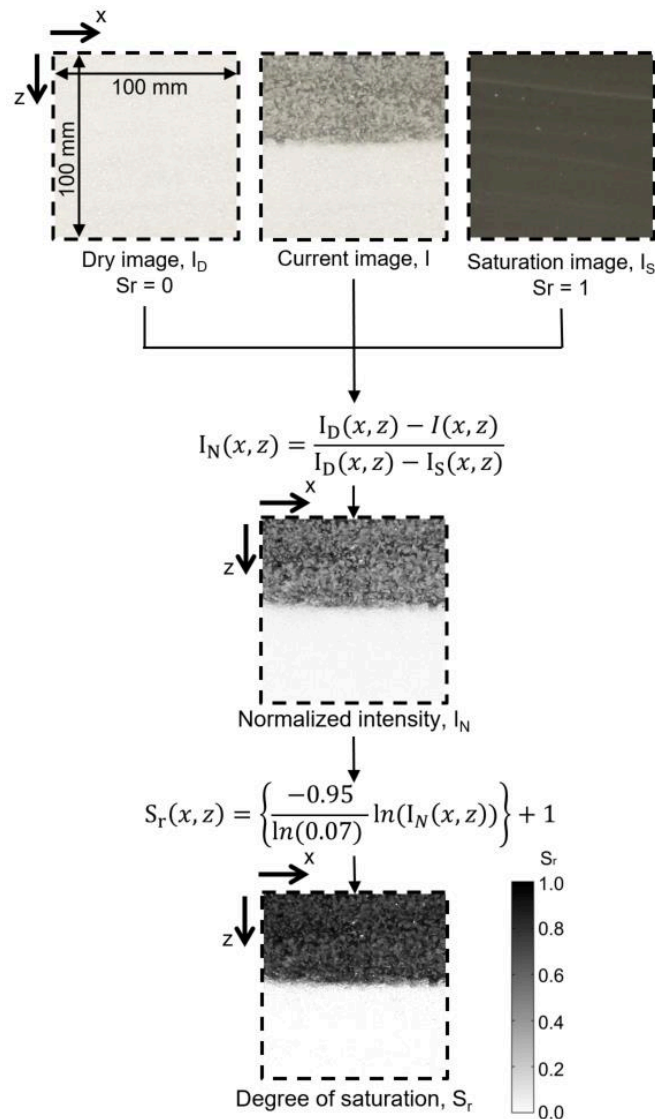


Figure 3. Schematic showing digital image analysis process from raw image to normalized intensity to degree of saturation.

SPATIAL RESOLUTION ON SATURATION MEASUREMENTS

Discussion of the spatial resolution of saturation measurements in unsaturated transparent soil experiments has both experimental interpretation and practical implications. Figure 4 shows the saturation image used to display the image analysis procedure with the highlighted area at the camera resolution, 0.3mm/measurement and reduced incrementally two orders of magnitude to 33.3mm/measurement. Images

were re-sized in Matlab to change the spatial resolution. The highlighted areas show the measurement size increases there is a corresponding loss of detail.

Experimental considerations which are affected by the spatial resolution include pore size distribution and local heterogeneities. Degree of saturation measurements at a spatial resolution less than the size of a pore are unreasonable. In the absence of microscopic analysis, a pore can only be filled or empty. The coarse gradation of transparent soil has $d_{10}=0.75\text{mm}$ and $d_{60}=1.175\text{mm}$, which coincide with anticipated pore sizes. This physical limit, of approximately 1mm, is contrasted with the thickness averaged nature of the saturation measurements as light passes through the 45mm thick soil and is captured on digital images. In any case, the d_{10} provides a practical minimum for spatial resolution of saturation measurements. Local heterogeneities can play an important role in flow regimes as they can cause local variability in hydraulic conductivity. To monitor local saturation variability, the spatial resolution must be restricted to a maximum size. In Figure 4, the large saturation image shows changes in colour associated with local layering of the test sample. Local layering is observable at the 0.33mm and 1mm. However, this detail is lost at larger spatial resolutions (2.5mm and greater). If layering is embedded in an unsaturated transparent soil experiment, several measurement points are needed within a layer to quantify local saturation variations. Otherwise, this potentially important detail could be lost.

Practical implications of selecting a spatial resolution for saturation measurements relate to availability of digital cameras. Two Canon XTi cameras are used in these experiments to capture soil behaviour (Camera 'C' in Figure 2 only records the balance reading). The entire apparatus could have been viewable through a single camera; however, the camera and available lens combination would not have provided 0.33mm pixel resolution viewable here. Locating cameras such that the combined images will be captured perfectly perpendicular is practically impossible. Following image processing, stitching together saturation images becomes a non-trivial task. Thus using a single camera lens combination to record the entire experiment is ideal if not always practical.

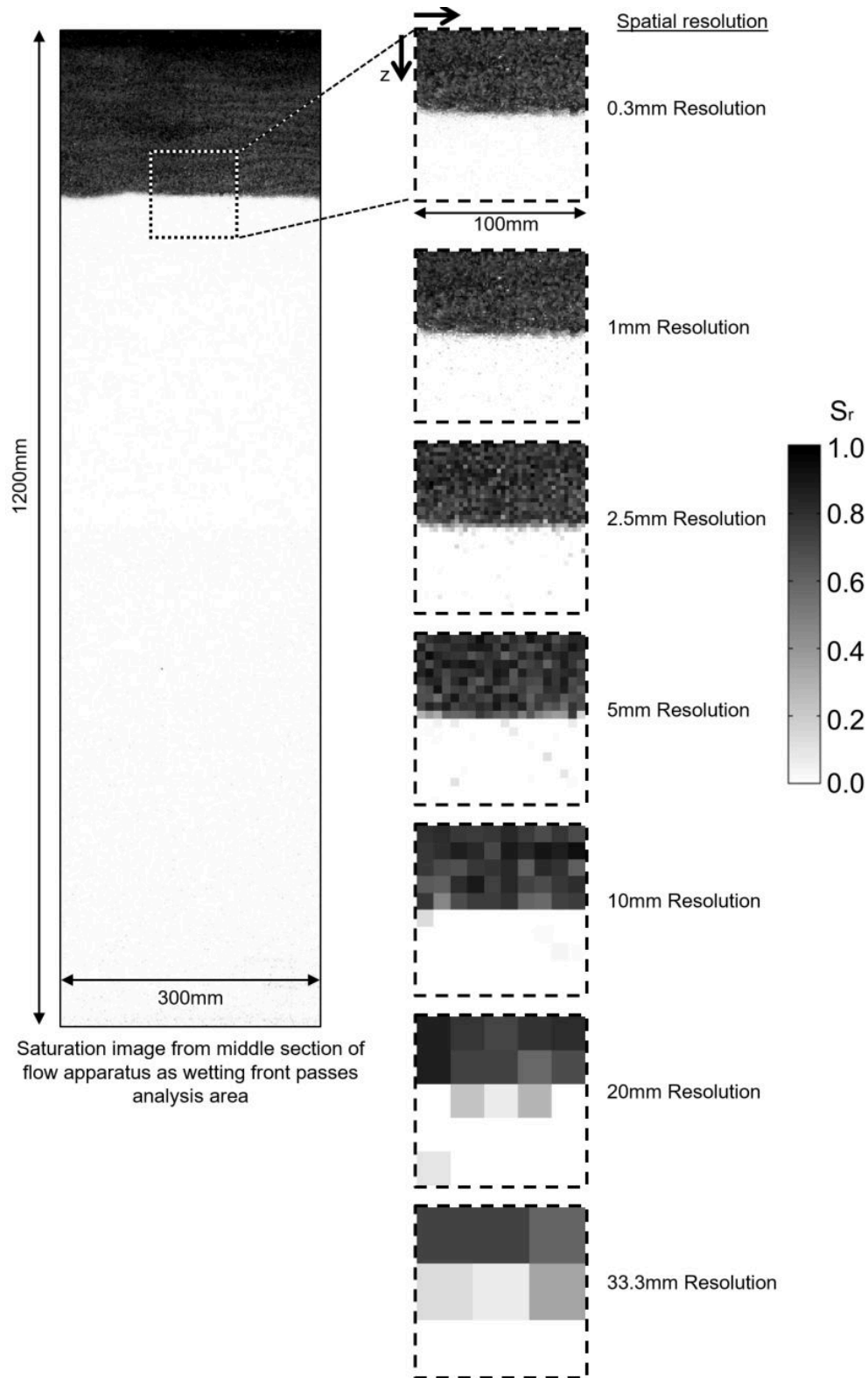


Figure 4. Effect of reducing degree of saturation spatial resolution two orders of magnitude from 0.3mm to 33.3mm for example analysis area.

An alternative to reducing the spatial resolution of a saturation image is to filter the image. Figure 5 displays the effects of filtering saturation images at spatial resolutions from 1-33.3mm as saturation images and vertical saturation profiles. Saturation images were filtered using a 5x5 pixel averaging function in Matlab. The resulting saturation image averages saturation measurements with adjacent pixels. The effect is to further smooth out local saturation variations. Layers clearly visible at 1mm and 2.5mm resolution become blurry and non-distinguishable at larger resolutions. A second effect is the accuracy and precision of locating the wetting front from saturation profiles. On the right side of Figure 5, saturation profiles are shown at resolutions from 1-33.3mm. The plots from 1-5mm resolution are virtually identical except for smoothing of local variations in the transmission zone above the wetting front. The wetting front location is clearly visible as the horizontal line where saturation decreases to zero at the same elevation as the colour change. At spatial resolutions of 10mm and larger the change in saturation at the wetting front becomes angled rather than flat. Accurate and precise locations of the wetting front are not possible.

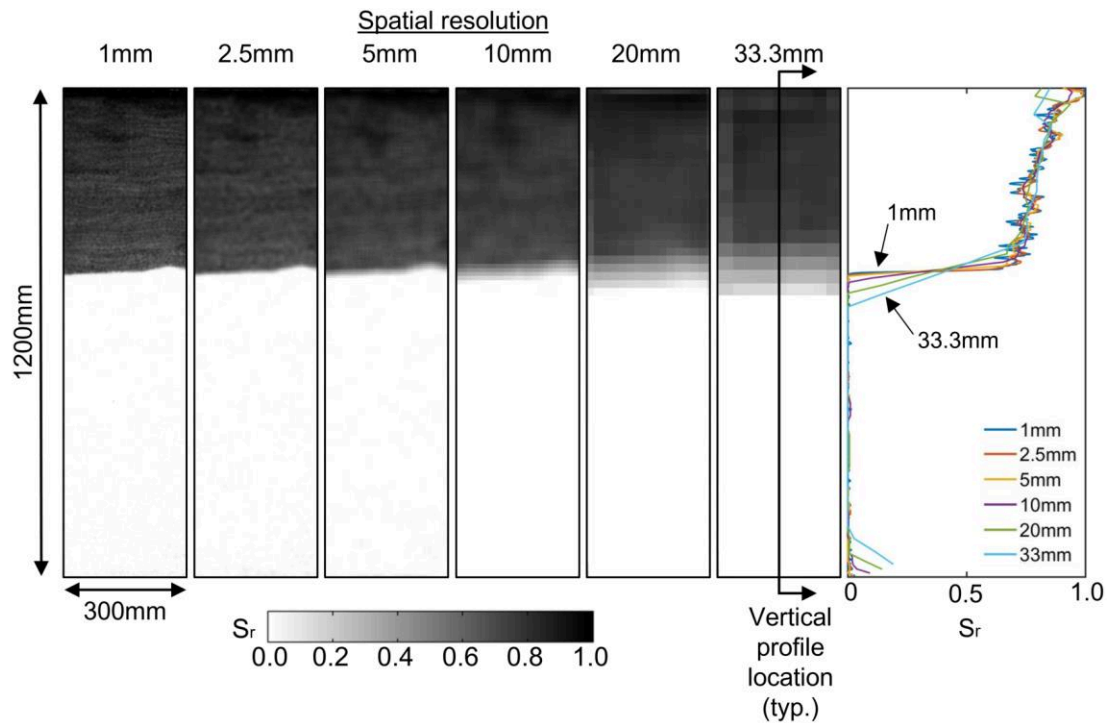


Figure 5. Effect of resolution and filtering on saturation measurements in two-dimensional saturation images and saturation profiles.

CONCLUSION

Unsaturated transparent soil experiments provide saturation measurements at spatial and temporal resolutions orders of magnitude higher than traditional instrumentation. At 1mm resolution, this method provides over 10^6 saturation measurements for each image of the 1200x1400mm size flow apparatus. This paper presented the two-dimensional flow apparatus, the digital image analysis process and discussed the effect of spatial resolution and filtering on saturation measurements. For the continuous flow experiments reported here, guidance is given to limit the spatial resolution to the minimum pore size of interest. Maximum spatial resolution is dependent on the number of local layers of interest as well as the need to accurately and precisely locate the wetting front. For the coarse gradation, experimental results shown here the minimum limit is 1mm and maximum is 5 mm. Other practical implications are the available digital camera and lens combination as use of additional cameras increases complexity of the analysis.

Use of transparent soil and the digital image processing method allows for investigation of a wide range of unsaturated flow behavior. With spatial resolution on the order of millimeters, continuous and discontinuous flow mechanisms can be investigated. The nonlinear and discrete behavior predicted by unsaturated soil inputs and numerical simulations can now be observed directly. Effects of local heterogeneities on flow regimes as well as behavior of capillary breaks with accurate measurements of the displacement distance are possible with this technology. Future work will consider both these continuous flow applications as well as discontinuous air injection experiments.

REFERENCES

- Fredlund, D. G. (2006). Unsaturated soil mechanics in engineering practice. *Journal of Geotechnical and Geoenvironmental Engineering*, 132(3), 286-321.
- Fredlund, D. G., & Morgenstern, N. R. (1976). Constitutive relations for volume change in unsaturated soils. *Canadian Geotechnical Journal*, 13(3), 261-276.
- Fredlund, D. G., & Morgenstern, N. R. (1977). Stress state variables for unsaturated soils. *Journal of Geotechnical and Geoenvironmental Engineering*, ASCE 103.
- Fredlund, D. G., Morgenstern, N. R., & Widger, R. A. (1978). The shear strength of unsaturated soils. *Canadian Geotechnical Journal*, 15(3), 313-321.
- Fredlund, D.G., Rahardjo, H.G., & Fredlund, M.D. (2012). *Unsaturated Soil Mechanics in Engineering Practice*, Wiley, New York
- Fredlund, D. G., & Xing, A. (1994). Equations for the soil-water characteristic curve. *Canadian Geotechnical Journal*, 31(4), 521-532.
- Fredlund, D. G., Xing, A., & Huang, S. (1994). Predicting the permeability function for unsaturated soils using the soil-water characteristic curve. *Canadian Geotechnical Journal*, 31(4), 533-546.

- Peters, S.B., Siemens, G., & Take, W.A. (2011). Characterization of transparent soil for unsaturated applications. *ASTM Geotechnical Testing Journal*, 34(5): 445-456.
- Vanapalli, S. K., Fredlund, D. G., Pufahl, D. E., & Clifton, A. W. (1996). Model for the prediction of shear strength with respect to soil suction. *Canadian Geotechnical Journal*, 33(3), 379-392.
- Sheng, D., Fredlund, D. G., & Gens, A. (2008). A new modelling approach for unsaturated soils using independent stress variables. *Canadian Geotechnical Journal*, 45(4), 511-534.
- Siemens, G.A. (2016). Thirty-ninth Canadian Geotechnical Colloquium: Unsaturated Soil Mechanics: Bridging the Gap Between Research and Practice. *In review*. Canadian Geotechnical Journal (December 2016, MS#cgj2016-0709).
- Siemens, G.A. and Oldroyd, C.P. (2014). Comparison of 1D and 2D infiltration results using unsaturated transparent soil, *UNSAT 2014, Unsaturated Soils: Research & Applications*, Sydney Australia 2-4 July 2014 Vol. 2, 1085-1090.
- Siemens, G.A., Peters, S.B. and Take, W.A. (2013). Comparison of confined and unconfined infiltration in transparent porous media. *Water Resources Research*. 49: 851-863
- Siemens, G.A., Take, W.A. & Peters, S.B. (2014). Physical and numerical modeling of infiltration including consideration of the pore air phase. *Canadian Geotechnical Journal*, 51: 1475–1487
- Sills, L-A.S., Mumford, K.G., & Siemens, G.A. (2017). Quantification of fluid saturations in transparent porous media. *Vadose Zone Journal*, 16(2), 2-9.
- White, D. J., Take, W. A., & Bolton, M. D. (2003). Soil deformation measurement using particle image velocimetry (PIV) and photogrammetry. *Geotechnique*, 53(7), 619-632.
- Wilson, G. W., Fredlund, D. G., & Barbour, S. L. (1994). Coupled soil-atmosphere modelling for soil evaporation. *Canadian Geotechnical Journal*, 31(2), 151-161.
- Wilson, G. W., Fredlund, D. G., & Barbour, S. L. (1997). The effect of soil suction on evaporative fluxes from soil surfaces. *Canadian Geotechnical Journal*, 34(1), 145-155.

Microstructure and Shear Strength of Widely Graded Soils during Desaturation

Hongfen Zhao¹ and Limin Zhang, F.ASCE²

¹Faculty of Civil Engineering and Geosciences, Delft Univ. of Technology, Stevinweg 1, 2628 CN, Delft, Netherlands. E-mail: H.Zhao@tudelft.nl

²Professor, Dept. of Civil and Environmental Engineering, Hong Kong Univ. of Science and Technology, Clear Water Bay, Hong Kong (corresponding author). E-mail: cezhangl@ust.hk

Abstract

The fabric, water retention curves (WRC) and shear strength of a fines-controlled soil, a coarse-controlled soil and a transitional soil were investigated through laboratory tests. The pore size distribution (PSD) and WRC of the fines-controlled soil show unimodal features dominated by intra-aggregate pores. During the desaturation process, the fines-controlled soil shrunk as water gradually drained from the intra-aggregate pores. The apparent peak and critical cohesions increased gradually with suction. For the coarse-controlled soil, its PSD and WRC exhibited bimodal features. Accordingly, the shear strength over the entire suction range also showed two distinct modes. The pore water drained from the inter-aggregate pores in the first mode while the intra-aggregate pores remained saturated. The apparent critical cohesion reached a peak and then decreased with increasing suction. The apparent critical cohesion increased again as the clay aggregates became unsaturated in the second mode. However, the apparent peak cohesion kept increasing with suction. The transitional soil exhibited weak bimodal features in its PSD and WRC, and was strongly contractive when saturated as the clay aggregates tended to collapse into the large inter-aggregate pores.

INTRODUCTION

The soil fabric changes with the coarse content in the soil. Zhao et al. (2013a) observed that clay aggregates form the skeleton of a fines-controlled soil, and that coarse-controlled specimens form a skeleton with grain to grain contacts, with the fine particles partially filling the large inter-particle pores. The structure of a soil in between (i.e. a transition soil) is controlled by clay aggregates and coarse particles together. The water retention curve (WRC) is controlled by its microporosity structure. A unimodal WRC was observed for Kaolin clay and clean Ottawa sand (Thu et al. 2007; Likos et al. 2012), while bimodal WRCs with two air-entry suctions were reported by Burger and Shackelford (2001), Zhang and Chen (2005), Li et al. (2009), Li and Zhang (2009), Zhang and Li (2010), Zhao et al. (2013b) and others.